Reciprocal Binary Mixture of Protic/Aprotic Ionic Liquids as Deep Eutectic Solvent: Physicochemical Behaviour and Application towards Agarose Processing

Pankaj Bharmoria,[1] Krishnaiah Damarla,[1] Tushar J. Trivedi,[1] Naved I Malek[2] and Arvind Kumar*[1,3]

[1]*Academy of Scientific and Innovative Research, CSIR-Central Salt and Marine Chemicals Research Institute, Salt and Marine Chemicals Division, G. B. Marg, Bhavnagar-364002, India,*

[2]*Applied Chemistry Department, S.V. National Institute of Technology, Surat- 395 007, India.*

[3]*Salt and Marine Chemicals Division, CSIR-Central Salt and Marine Chemicals Research Institute, G. B. Marg, Bhavnagar-364002, India.*

.

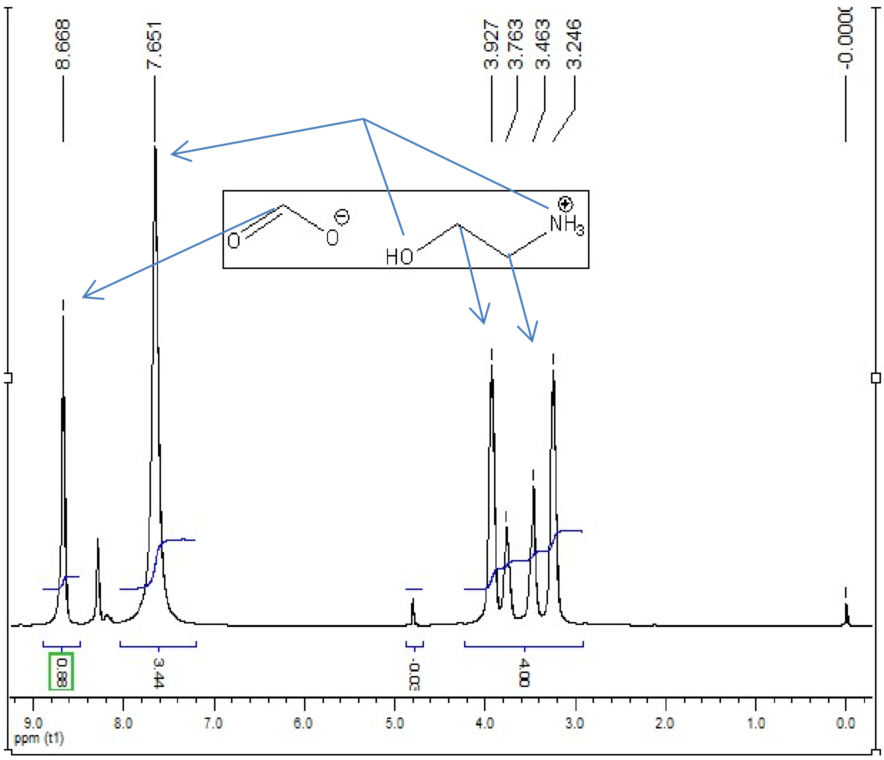

Fig. S1. ^{1}H-NMR spectra of [HEA][HCOO] ionic liquid. The absence of ^{1}H-NMR peak of the O-H of formic acid at 2 *ppm* and NH_2 of ethanolamine at 5 *ppm* in the prepared IL confirms the absence of any free acid or base.

Fig. S2. ^{13}C-NMR spectra of [HEA][HCOO] ionic liquid.

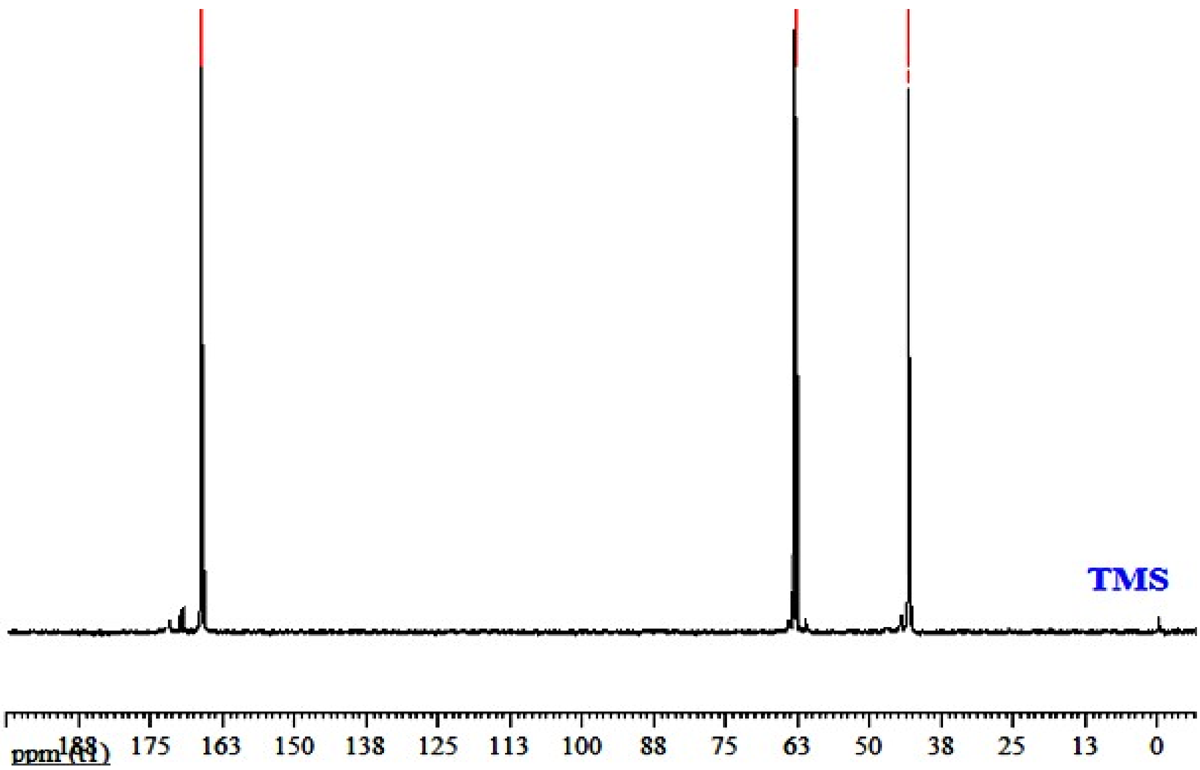

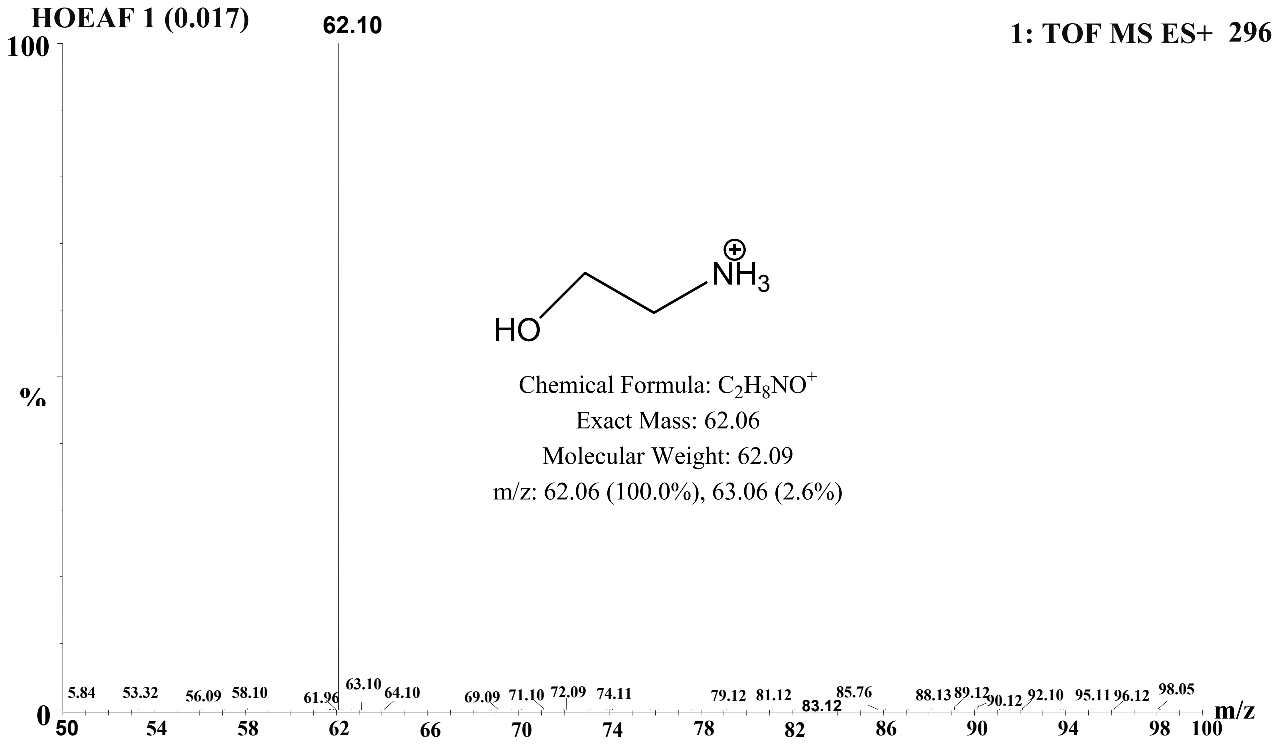

Fig. S3. LCMS spectra of [HEA][HCOO] ionic liquid.

CHNS Analysis of [HOA][HCOO]

Theoretical	Experimental
C=33.64%	C =35±0.5%
H=8.47%	H = 8%±0.5%
N=13.08%	N=14.50±0.5%

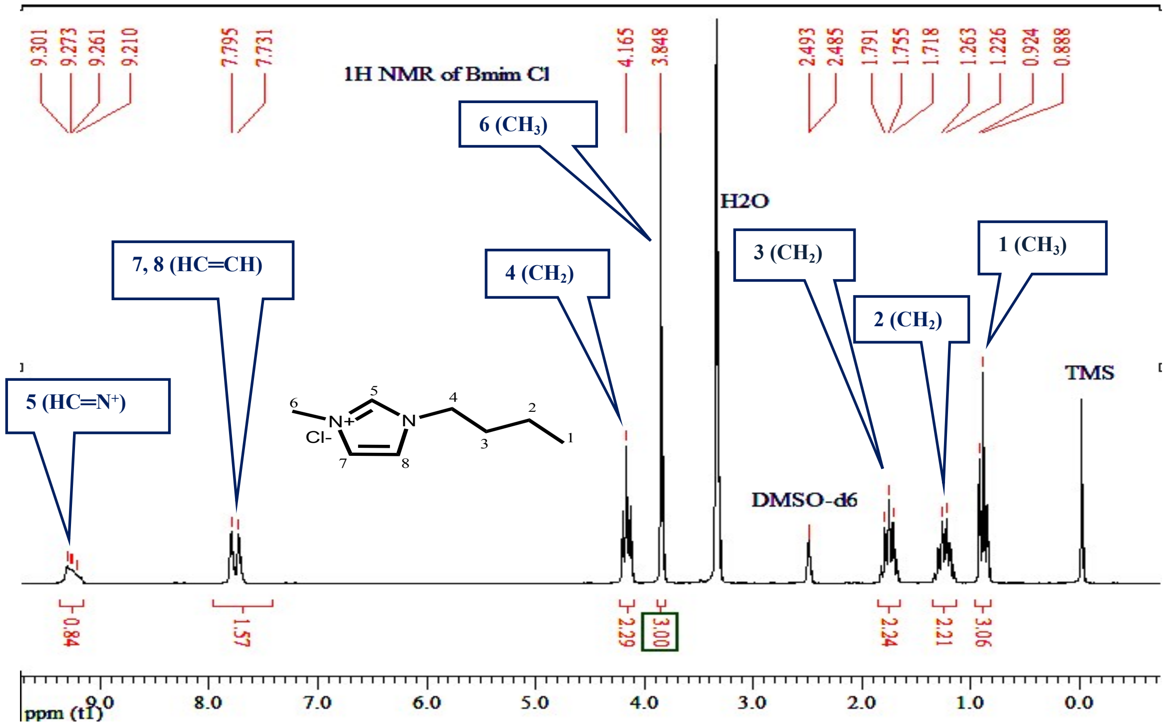

Fig. S4. ^{1}H-NMR spectra of $[C_4mim][Cl]$ ionic liquid.

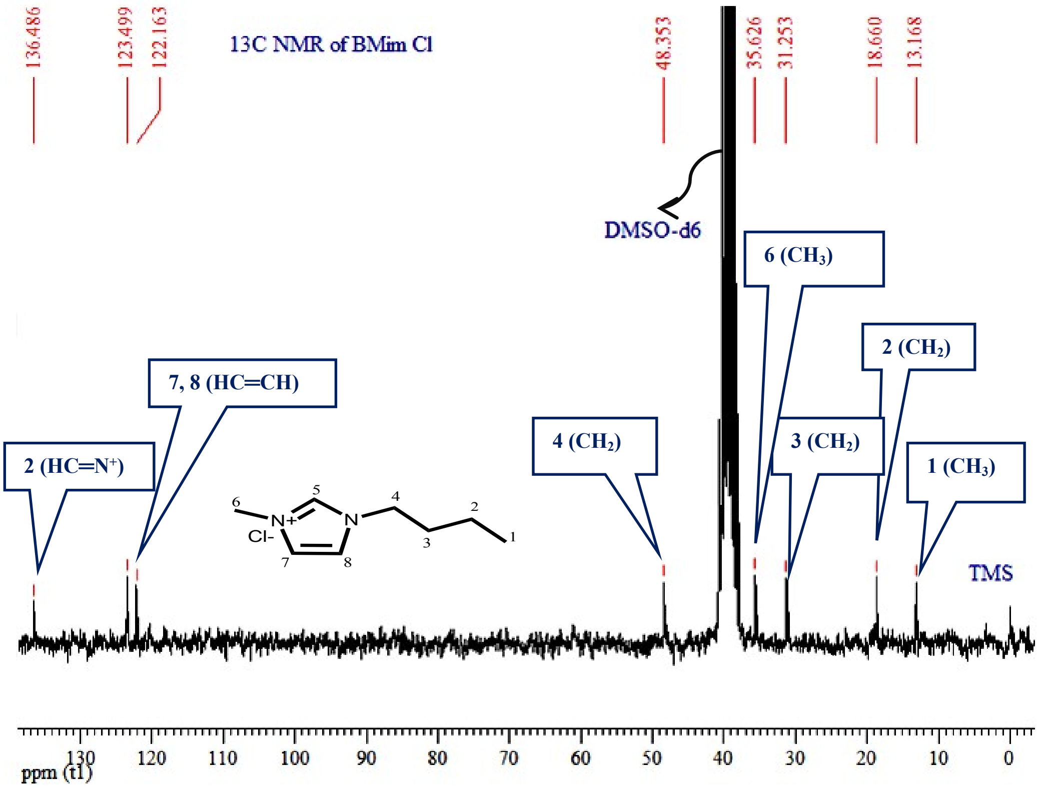

Fig. S5. ^{13}C-NMR spectra of $[C_4mim][Cl]$ ionic liquid.

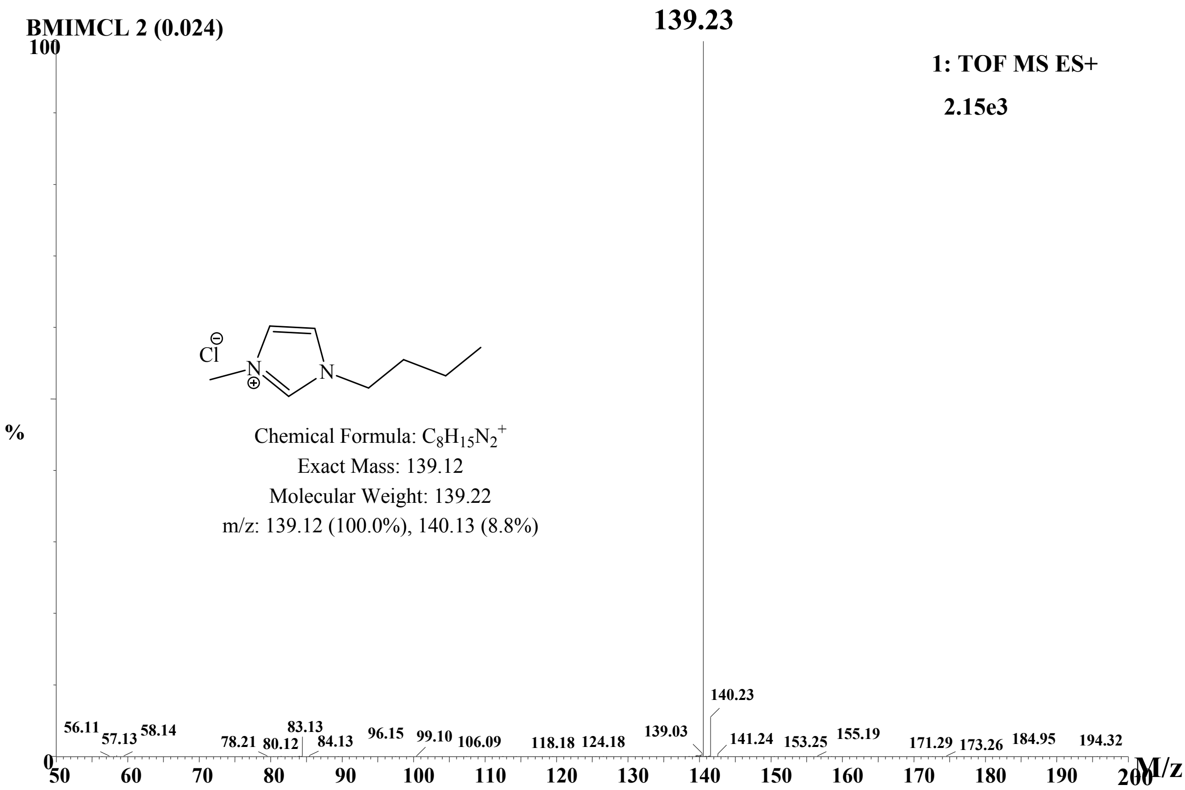

Fig. S6. LCMS Spectra of $[C_4mim][Cl]$ ionic liquid.

Fig. S7. Visual Images of [C_4mim][Cl]+[HEA][HCOO] eutectic mixtures at different mixture compositions

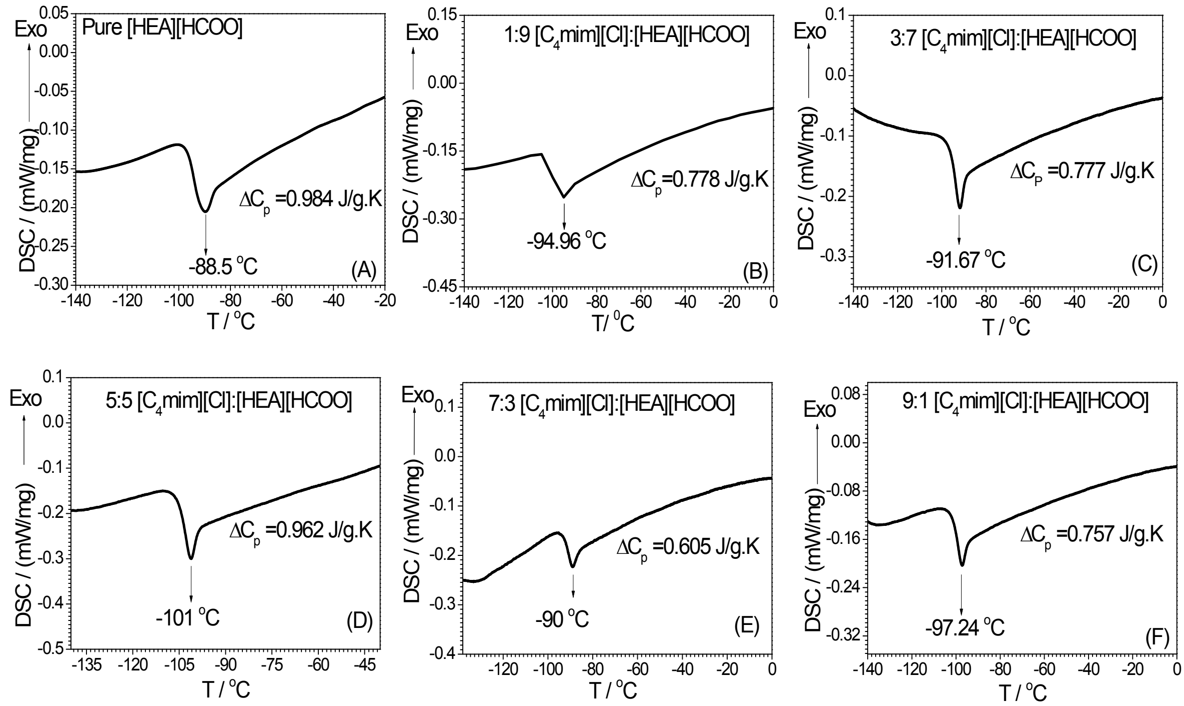

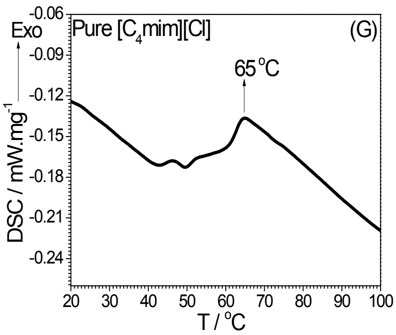

Fig. S8. DSC thermograms (A) Pure [HEA][HCOO] (B-F) [C_4mim][Cl]+[HEA][HCOO] mixtures at different mixture compositions (G) pure [C_4mim][Cl].

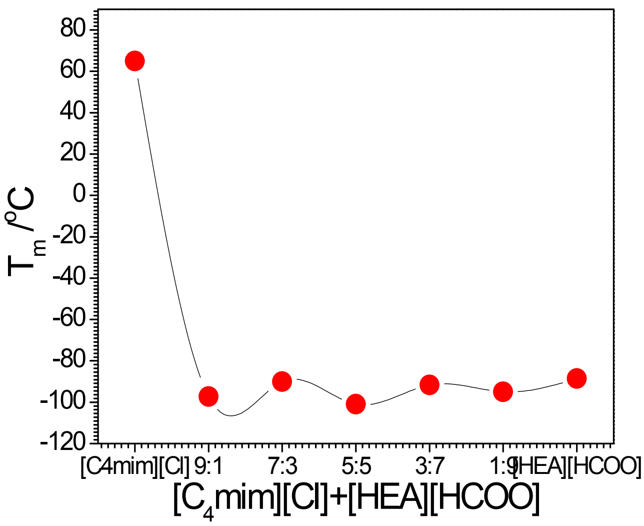

Fig. S9. Plots showing the melting points of [C$_4$mim][Cl] + [HEA][HCOO] mixtures and native [C$_4$mim][Cl] and [HEA][HCOO].

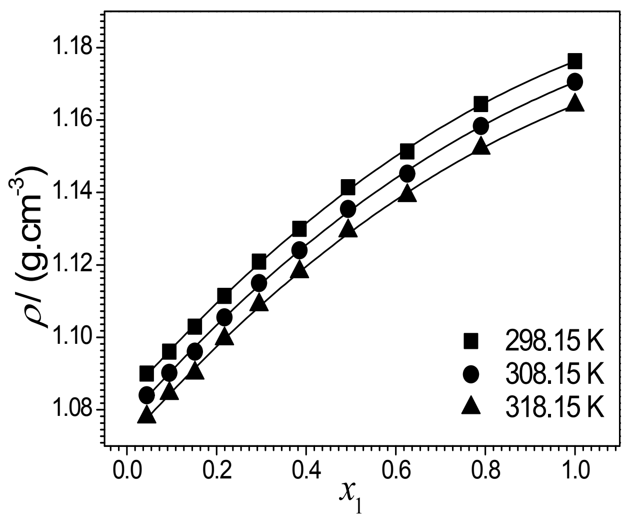

Fig. S10. Plots of variation in density of [HEA][HCOO] (x_1)+[C$_4$mim][Cl] (x_2) mixture at different mole fractions at 298.15 K, 308.15 K, and 318.15 K.

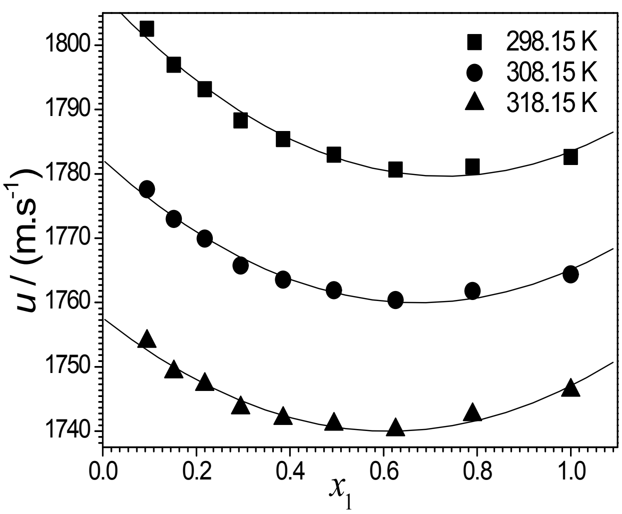

Fig. S11. Variation in speed of sound (u) of [HEA][HCOO] (x_1)+[C_4mim][Cl] (x_2) mixture at different mole fractions at 298.15 K, 308.15 K, and 318.15 K.

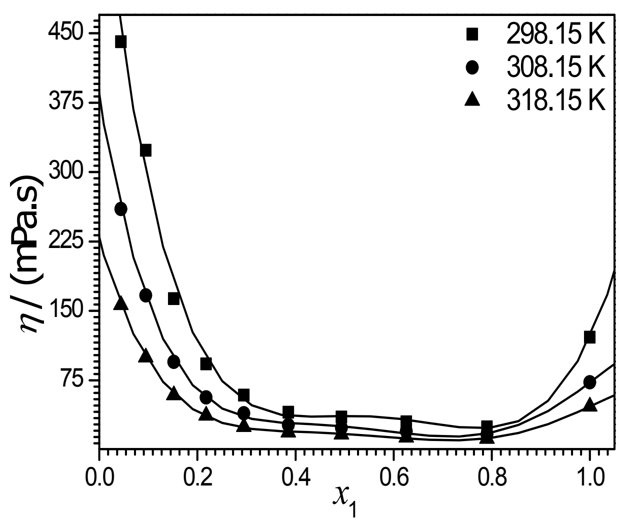

Fig. S12. Variation in viscosity (η) of [HEA][HCOO] (x_1)+[C_4mim][Cl] (x_2) mixture at different mole fractions at 298.15 K, 308.15 K, and 318.15 K.

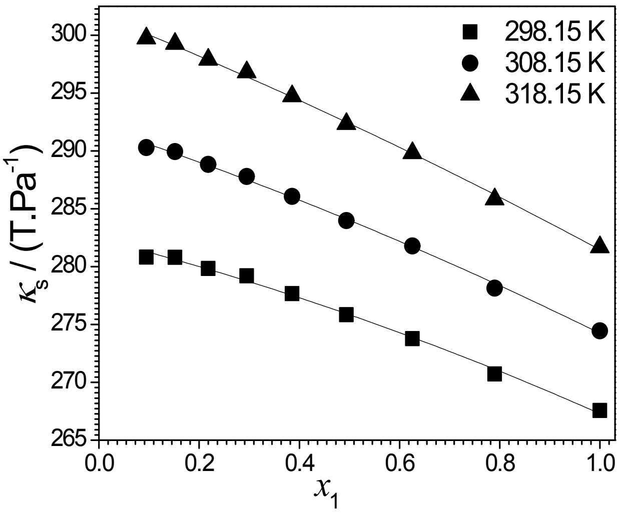

Fig. S13. Variation in isentropic compressibility (κ_s) of [HEA][HCOO](x_1)+[C_4mim][Cl](x_2) at different mole fractions at 298.15 K, 308.15 K and 318.15 K.

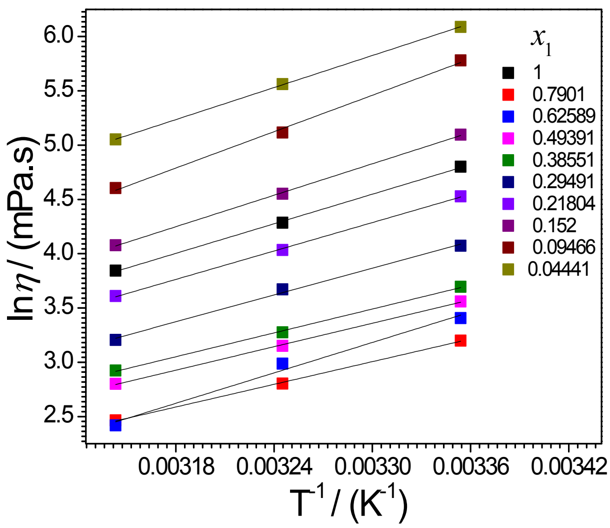

Fig. S14. Arrhenius plots (lnη vs T^{-1}) showing variation in viscosity as a function of temperature for [HEA][HCOO](x_1) + [C_4mim][Cl](x_2) mixtures at different mole fractions

Table S1. Experimental Kamlet-Taft parameters of [HEA][HCOO](x_1)+[C_4mim][Cl] (x_2) mixtures at various mole fractions of [HEA][HCOO] at 298.15 K.

x_1	Polarity Parameters				
	$E_T(30)$ (kCal. mol^{-1})	E_N^T (kCal.mol^{-1})	π^*	α	β
0.04441	51.33	0.6309	1.11	0.49	0.83
0.152	54.05	0.71398	1.08	0.69	0.79
0.29491	56.28	0.78231	1.02	0.87	0.76
0.49391	57.76	0.82751	1.04	0.94	0.71
0.7901	58.11	0.83828	1.06	0.95	0.67
1	58.35	0.84553	1.08	0.96	0.62

Table S2. Experimental values of wavelengths corresponding to absorption maximum of nitroaniline (4NA), Reichardt's dye (RD) and N-N-diethylnitoaniline (DENA) [HEA][HCOO](x_1) + [C_4mim][Cl] (x_2) mixtures at various mole fractions of [HEA][HCOO] at 298.15 K.

x_1	λ_{max} (nm)		
	RD	*4NA*	*DENA*
0.04441	557	398	417
0.152	529	394	415
0.29491	508	390	412
0.49391	495	389	413
0.7901	492	388	414
1	490	387	415

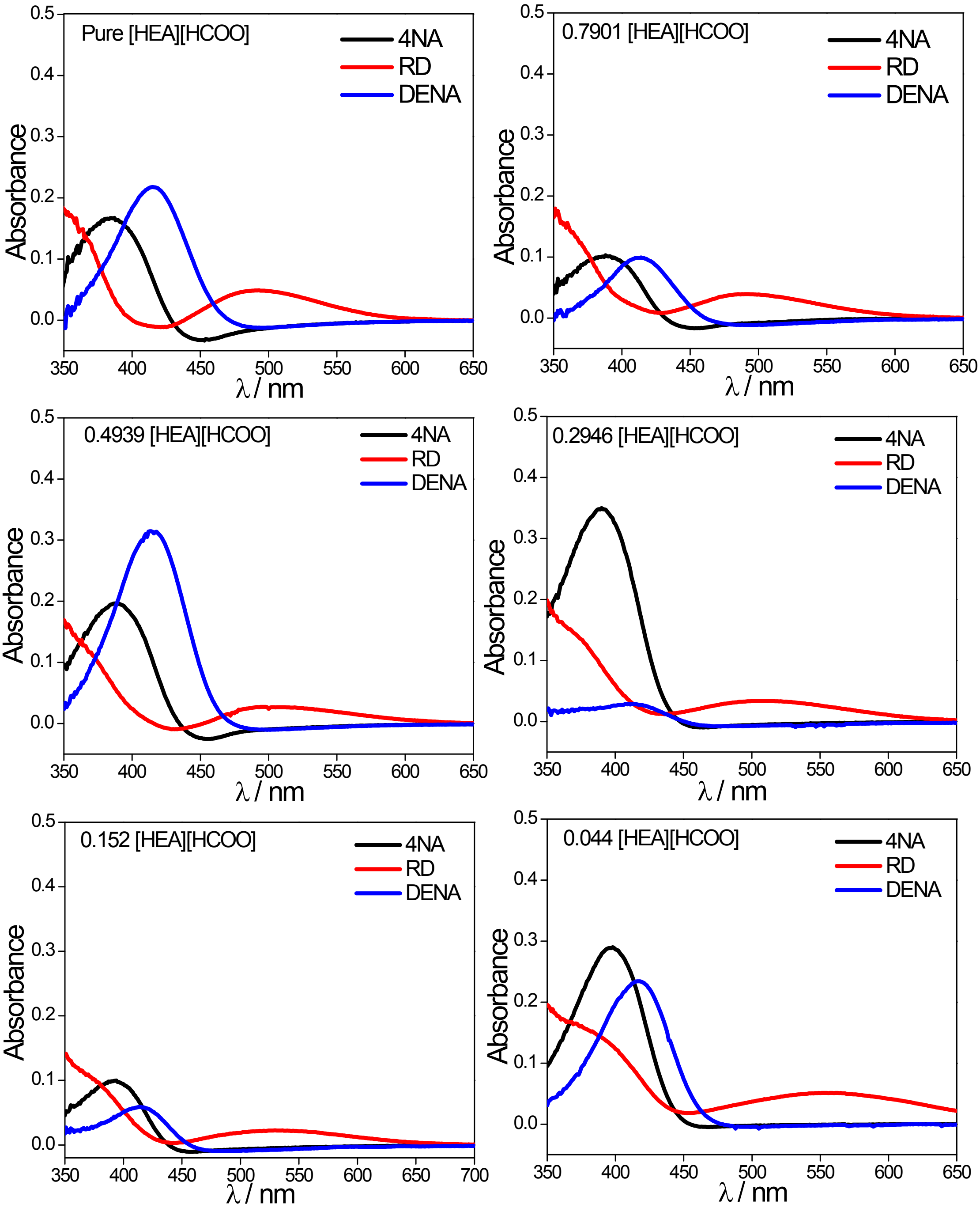

Fig. S15. UV-Vis spectra of the dyes, nitroaniline (4NA), Reichardt's dye (RD) and N-N-diethylnitoaniline (DENA) in the [HEA][HCOO](x_1)+[C_4mim][Cl] (x_2) mixtures at various mole fractions.

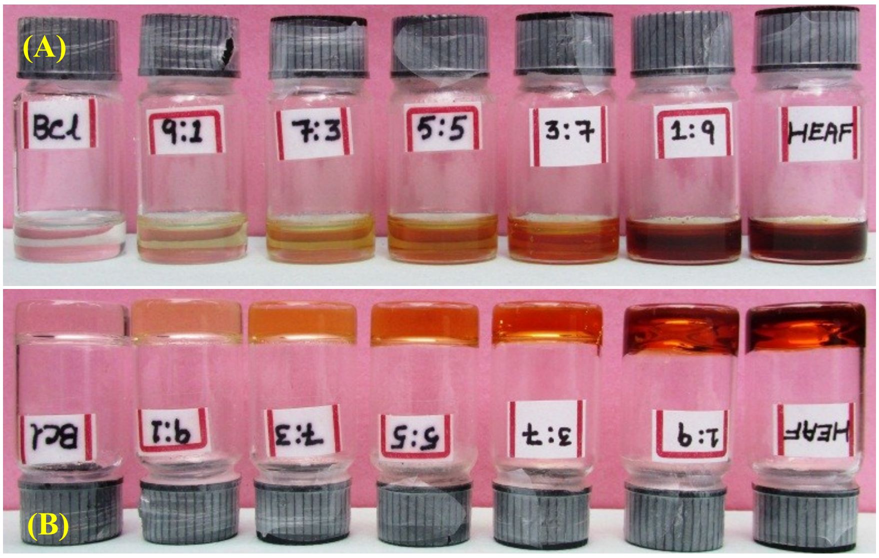

Fig. S16. (A) Ionosols of agarose dissolved in native [HEA][HCOO](x_1)+[C_4mim][Cl] mixtures and native ILs at 70°C. (B) Agarose ionogels prepared by cooling the ionosols to room temperature.

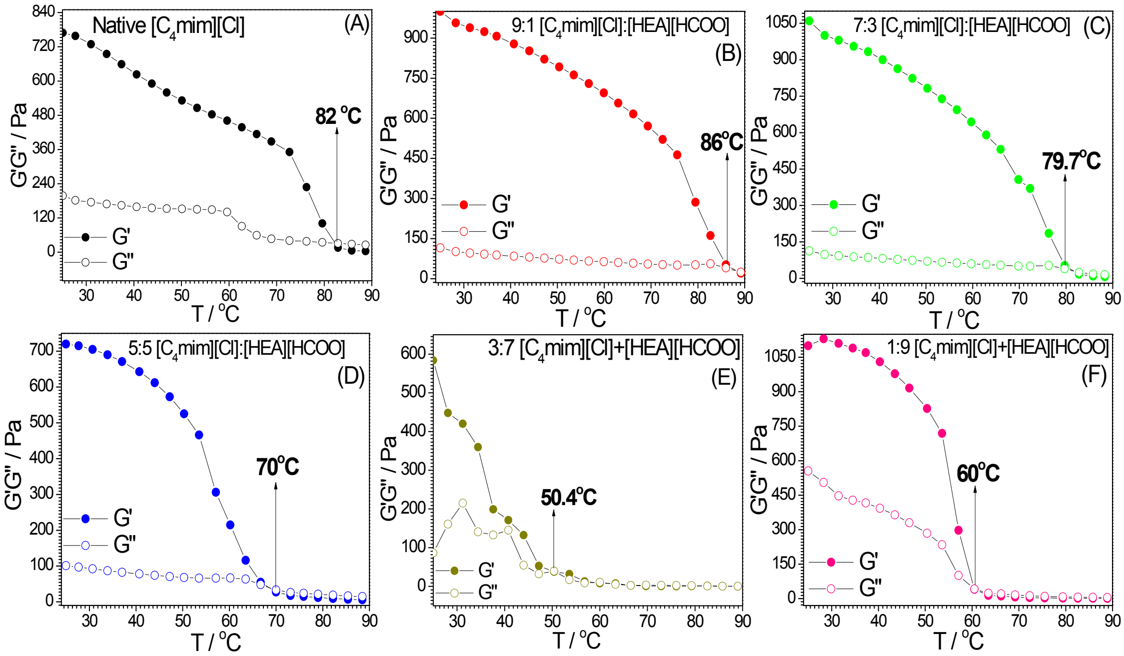

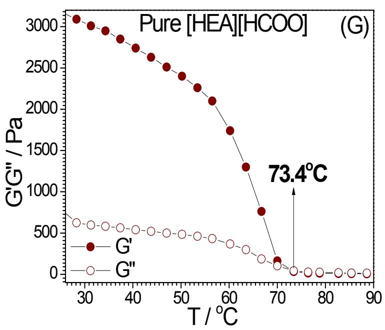

Fig. S17. Plot showing dynamic storage (G') and loss moduli (G") vs temperature profiles of ionogels prepared by dissolving 5% agarose in different mixture compositions of [C_4mim][Cl]+[HEA][HCOO]. The crossing point of G' and G" indicating the melting temperature.

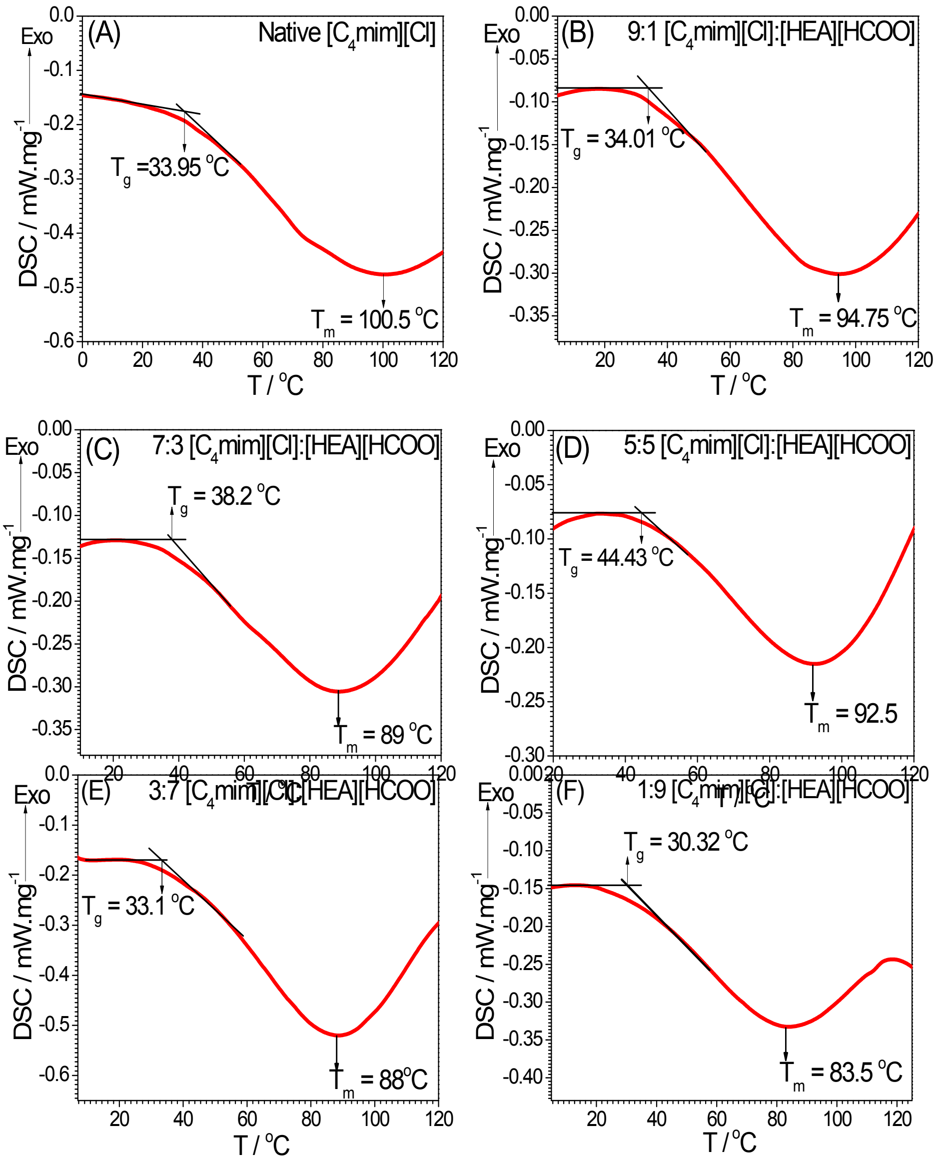

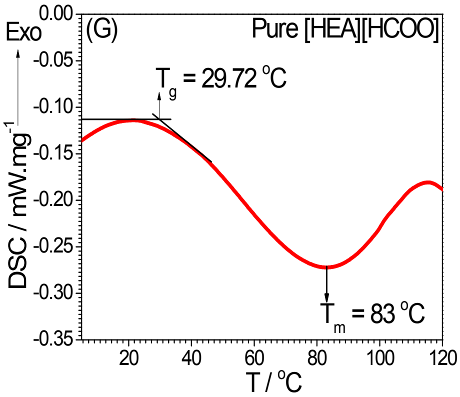

Fig. S18. Plot showing DSC thermograms of agarose ionogels prepared in different composition of [C_4mim][Cl]+[HEA][HCOO].

Table S3. Glass transition (T_g) and Meting temperatures (T_m) of *agarose* ionogels measured from DSC and temperature dependent rheology measurements.

5% Agarose Gels in the Ionic Liquid Mixtures	Glass transition Temp. DSC (T_g / °C)	Melting Temp. DSC (T_m / °C)	Melting Temp. Rheology (T_m / °C)
Native [C_4mim][Cl]	33.95	100.5	82.00
9:1 [C_4mim][Cl]+[HEA][HCOO]	34.01	94.75	86.00
7:3 [C_4mim][Cl]+[HEA][HCOO]	38.20	89.00	79.70
5:5 [C_4mim][Cl]+[HEA][HCOO]	44.43	92.50	70.00
3:7 [C_4mim][Cl]+[HEA][HCOO]	33.10	88.00	56.80
1:9 [C_4mim][Cl]+[HEA][HCOO]	30.32	83.50	60.00
9:1 [HEA][HCOO]	29.72	83.00	73.40

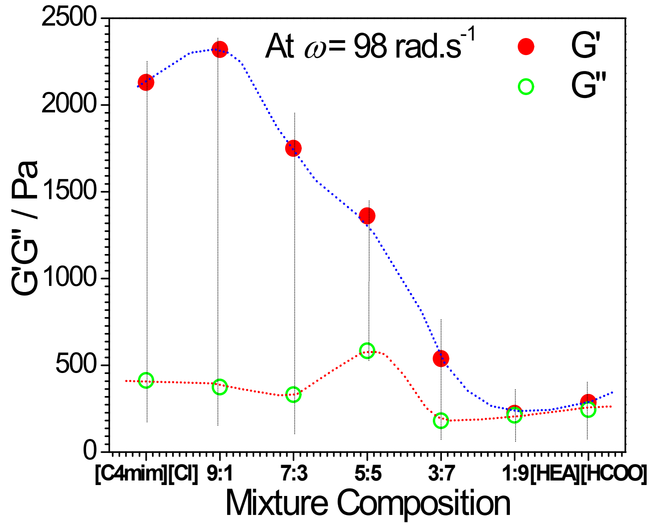

Fig. S19. Comparative plot of the G' and G" of ionogels formed at different mole fractions at an angular frequency of 98 rad.s^{-1}

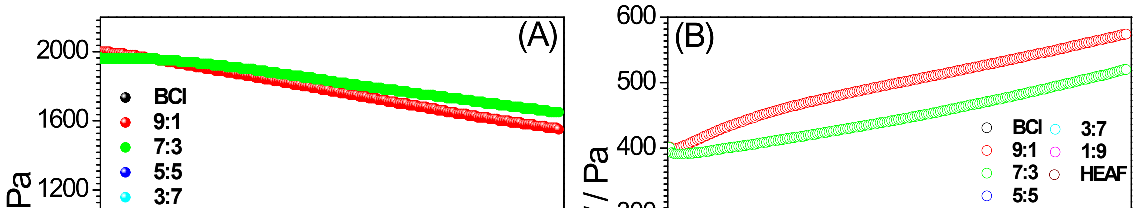

Fig. S20. Strain (γ%) dependence of (A) dynamic storage (G') and (B) loss moduli (G") of agarose ionogels (5%) at different compositions of [C_4mim][Cl]+[HEA][HCOO].

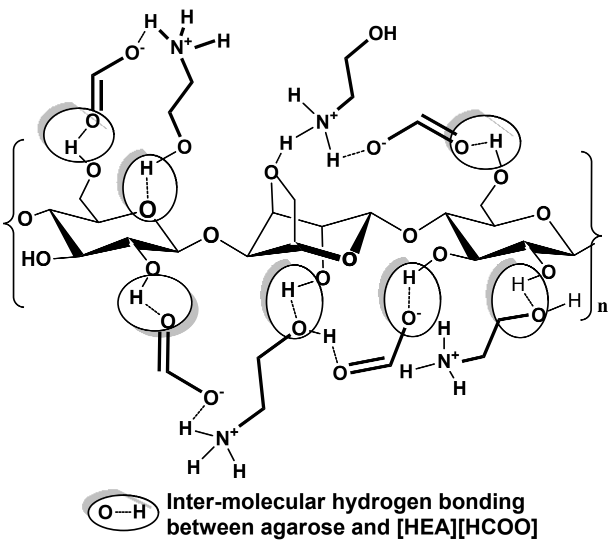

Fig. S21. Schematic showing inter-molecular hydrogen bonding between *agarose* and [HEA][HCOO].